# NATIONAL ADVISORY COMMITTEE FOR AERONAUTICS

## TECHNICAL NOTE 4357

LIFT AND PROFILE-DRAG CHARACTERISTICS OF

AN NACA 0012 AIRFOIL SECTION AS DERIVED FROM MEASURED

HELICOPTER-ROTOR HOVERING PERFORMANCE

By Paul J. Carpenter

Langley Aeronautical Laboratory
Langley Field, Va.

NACA

Washington

September 1958

NATIONAL ADVISORY COMMITTEE FOR AERONAUTICS

TECHNICAL NOTE 4357

LIFT AND PROFILE-DRAG CHARACTERISTICS OF

AN NACA 0012 AIRFOIL SECTION AS DERIVED FROM MEASURED

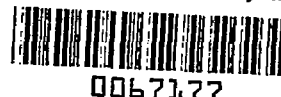HELICOPTER-ROTOR HOVERING PERFORMANCE

By Paul J. Carpenter

SUMMARY


Synthesized rotor-blade section lift and profile-drag characteristics for an NACA 0012 airfoil section as a function of angle of attack and Mach number for use in calculations of helicopter-rotor hovering performance are presented. Measured rotor hovering performance from which the major portion of the synthesized data was derived is presented for a range of tip Mach numbers from 0.28 to 0.70. The synthesized data presented for Mach numbers from 0.70 to 0.88 were derived from a previous investigation of another blade having an NACA 0012 airfoil section at the tip.

At low tip Mach numbers the synthesized data have higher maximum lift and lower profile drag at maximum lift than the equivalent two-dimensional-airfoil data. At high tip Mach numbers, the rate of increase of drag due to compressibility is less than that shown by the two-dimensional-airfoil data.

The rotor-hovering-performance characteristics are similar to those shown by previously reported investigations at high tip Mach numbers. The principal effect of increased tip Mach number is a large profile-drag rise which occurs at progressively lower blade mean lift coefficients.


INTRODUCTION


Current helicopter trends toward increased speed and higher disk loadings have resulted in increased rotational tip speeds. As a result of these increased tip speeds, power increases and blade pitching moments due to compressibility effects have become as important as stall on the retreating blade in determining the maximum forward speed of the helicopter.

A numerical-integration method which may be used in calculating stall and compressibility effects in forward flight has been presented

in reference 1. The accuracy of such calculations depends on the validity of using two-dimensional airfoil-section data for helicopter performance. It has been found (at least in the hovering case in refs. 2 and 3) that using two-dimensional airfoil-section data results in underestimating low tip Mach number maximum lift and in overestimating the compressibility drag rise. Two reasons for these discrepancies are apparent: first, the blade boundary layer is subjected to centrifugal pumping, and, second, the blade has a finite span and is thus subject to the drag-alleviating effects of three-dimensional flow at the blade tip.

In order to provide more representative airfoil data for use in rotor-performance calculations, a general research program to synthesize airfoil-section lift and drag characteristics has been undertaken. The synthesized data are derived from measured hovering performance of a rotor tested on the Langley helicopter test tower and are presented herein for the NACA 0012 airfoil section. Although the synthesized data are derived from rotor hovering performance, it can reasonably be assumed (until proven otherwise) that the data are equally applicable to forward-flight calculations.

The measured rotor performance used in the synthesis of the major portion of the data (with blade tip Mach numbers from 0.28 to 0.70) is also presented and compared with the performance of blades having NACA $63_2$-015 and NACA 0015 airfoil sections. The synthesized data were extended to a Mach number of 0.85 by using the measured rotor performance over a tip Mach number range from 0.70 to 0.88 obtained with a blade having an NACA 0018 airfoil section at the root which tapered to an NACA 0012 airfoil section at the tip (ref. 4).

## SYMBOLS

a      slope of section-lift-coefficient curve as a function of section angle of attack (radian measure), assumed to be 5.73 for incompressible-flow calculations

b      number of blades

$C_m$      rotor-blade pitching-moment coefficient, $\dfrac{M_y}{\frac{R\rho}{2}(\Omega R)^2 c_e^2}$

$C_Q$      rotor torque coefficient, $\dfrac{Q}{\pi R^2 \rho (\Omega R)^2 R}$

$C_{Q,o}$       rotor profile-drag torque coefficient, $\dfrac{Q_o}{\pi R^2 \rho (\Omega R)^2 R}$

$C_T$       rotor thrust coefficient, $\dfrac{T}{\pi R^2 \rho (\Omega R)^2}$

$c$       blade-section chord at radius $r$, ft

$c_{d,o}$       airfoil-section profile-drag coefficient

$\Delta c_{d,o}$       incremental airfoil-section profile-drag coefficient

$c_e$       equivalent blade-section chord, $\dfrac{\displaystyle\int_0^R cr^2\,dr}{\displaystyle\int_0^R r^2\,dr}$, ft

$c_l$       airfoil-section lift coefficient

$\overline{c_l}$       rotor-blade mean lift coefficient, $6C_T/\sigma$

$c_t$       blade-tip-section chord, ft

$M$       Mach number

$\Delta M$       incremental Mach number

$M_t$       rotor-blade tip Mach number

$M_y$       rotor-blade pitching moment about $c/4$, lb-ft

$N_{Re}$       Reynolds number at blade tip, $\dfrac{\rho \Omega R c_t}{\mu}$

$Q$       rotor torque, lb-ft

$Q_o$       rotor profile-drag torque, lb-ft

$R$       rotor-blade radius, ft

$r$       radial distance to a blade element, ft

T          rotor thrust, lb

$\alpha$          airfoil-section angle of attack, deg or radians

$\alpha_{r,t}$        rotor-blade-tip angle of attack, deg or radians

$\theta$          blade-section pitch angle measured from line of zero lift,
             radians

$\mu$          coefficient of viscosity, slugs/ft-sec

$\rho$          mass density of air, slugs/cu ft

$\sigma$          rotor solidity,  $bc_e/\pi R$

$\Omega$          rotor angular velocity, radians/sec

Subscripts:

calc       calculated

meas       measured

The figure of merit is equal to  $0.707 \dfrac{c_T^{3/2}}{c_Q}$.


APPARATUS, TEST METHODS, AND ACCURACY


Rotor Blades

The rotor used for this investigation was a fully articulated, two-
blade rotor with the flapping hinge located on the center line of rota-
tion and the drag hinge located 12 inches (4.5-percent-radius station)
outboard of the center line. The distance from the ground to the rotor-
hub center was 42 feet. A photograph of the rotor installation on the
Langley helicopter test tower is shown in figure 1.

The rotor blades had a radius of 26.8 feet from the center of rota-
tion, a constant chord of 16.4 inches from 15 percent to 98 percent of
the blade radius, an NACA 0012 airfoil section, 8° of linear washout, and
a solidity of 0.0325. The tip cap was formed as shown in the following
sketch:

≈ 98-percent-radius
station
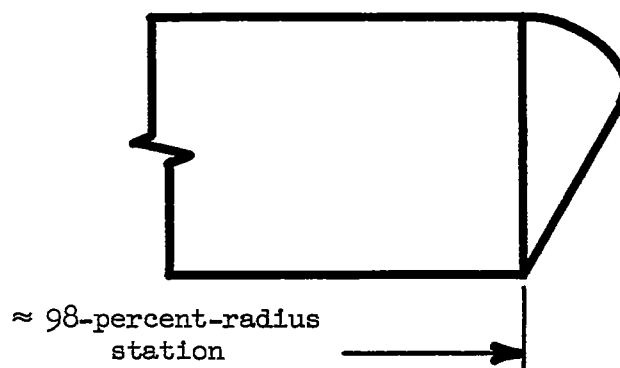
The rotor-blade surface forward of the 28-percent-chord station
was finished to true airfoil contour with tolerances of +0.000 and
-0.005 inch. The remaining part of the rotor blade deviated somewhat
more from the true airfoil, but was smooth and fair over most of the
area. The rearward portion of the rotor blade (about 3 percent of the
chord) could be deflected up or down a few degrees to provide a measure
of control over the rotor-blade pitching moments.

The blades had adjustable tip weights for spanwise and chordwise
balance. In order to reduce the blade lag angles encountered at high
pitch settings, part of the test program $\left(M_t = 0.28 \text{ to } 0.52\right)$ was made
by using 13.0-pound tip weights as compared with the normal tip weight
of 3.0 pounds.

## Test Methods and Accuracy

The tests were made by setting given rotor-blade collective pitch
angles and varying the rotor-shaft rotational speed through a range of
tip Mach numbers until either the limiting hub lag angle of $25°$ or the
limiting blade stress was reached. At low tip Mach numbers blade pitch
angles were limited to $18°$ or less because of the large lag angles.

At each pitch setting, data were recorded from visual dial readings
and by an oscillograph. Quantities measured were rotor thrust, rotor
torque, blade pitch angle, blade pitching moment, rotor-shaft rotational
speed, blade drag angle, and blade flapping angle.

The estimated accuracies of the basic quantities measured were as
follows:

Rotor thrust, lb . . . . . . . . . . . . . . . . . . . . . . . . . . . ±50
Rotor torque, lb-ft . . . . . . . . . . . . . . . . . . . . . . . . . ±50
Rotor-shaft rotational speed, rpm . . . . . . . . . . . . . . . . . . ±1
All angular measurements, deg . . . . . . . . . . . . . . . . . . . . ±0.2

The overall accuracy of the plotted results is believed to be within
±3 percent. For example, at a blade mean lift coefficient $\overline{c_l}$ of 0.81
and at $M_t = 0.48$, the accuracy of the data based on repeatability was
within ±1 percent for the thrust value of 8,254 pounds, ±1 percent for
the torque value of 11,022 pound-feet, and ±0.3 percent for a rotational-
speed value of 195.4 rpm.

## METHOD OF ANALYSIS

The derivation of airfoil-section data from the measured rotor per-
formance involves assuming airfoil-section characteristics, calculating
rotor characteristics, comparing calculated results with measured results,
and then adjusting the assumed airfoil-section properties in such a man-
ner that the calculated performance agrees closely with the measured per-
formance. Inasmuch as the method used in synthesizing such data has not
been previously explained in detail, the method will be discussed here
for reference purposes.

### Lift Characteristics

The first step in the synthesis is an approximation of the section
lift characteristics over the range of Mach numbers and angles of attack.
Considerable published data are available for guidance in arriving at
likely low Mach number (less than 0.1) characteristics (refs. 5, 6,
and 7). Guidance for the higher Mach number characteristics (0.3 to 0.85)
was obtained from unpublished data obtained in the Langley low-turbulence
pressure tunnel on the NACA 0012 airfoil section and from references 8
and 9. Reference 10 is useful as a guide in determining the variation
in maximum lift coefficients in the intermediate Mach number range
from 0.1 to 0.5. Another guide used in formulating the lift-curve
slopes as a function of Mach number is the Prandtl-Glauert relationship
which states that the lift-curve-slope increase is proportional to the
factor $\dfrac{1}{\sqrt{1 - M^2}}$.

The initial selections of section lift coefficient plotted against
Mach number and angle of attack are then used to calculate rotor thrust
as a function of blade pitch setting for the various tip Mach numbers.
The method used is the conventional strip analysis method given in ref-
erence 11, except that a tip loss factor has been introduced. The outer
3 percent of the blade radius is assumed to have profile drag but no
lift.

The calculation of the section angle of attack along the blade is dependent on the slope of the lift curve  a  as well as on the blade physical parameters. Since  a  is dependent of both angle of attack and Mach number, an iteration method is used in its determination. As a first assumption,  a  is given a value of 5.73 and section angles of attack along the blade span are calculated for several values of blade collective pitch. From these section angles of attack, the variation of  a  with angle of attack and Mach number is obtained by dividing the section lift coefficient (read from the synthesized data) by the angle of attack. The new values of  a  are then used to calculate a new span-wise section-angle-of-attack distribution. Usually, two such iterations are sufficient to define adequately the section angle of attack, that is, within $0.1^{\circ}$.

The section lift coefficients at the proper section Mach number and angle of attack are then inserted into the rotor-thrust equations, and the rotor thrust is calculated for the given collective blade pitch settings.

Next, the calculated rotor thrust is compared with the measured rotor thrust and, if necessary, modifications are made to the initial assumed section lift characteristics to make the calculated thrust agree with the measured thrust. Generally, three or four subsequent adjustments to the section-lift values, especially in the area of maximum lift coefficient, are required before agreement to within ±2 percent is reached.

### Section-Profile-Drag Characteristics

The same references used to guide the selection of lift characteristics are also used in section-profile-drag evaluation. In addition, it has been found that the conventional drag polar (ref. 12)

$$c_{d,o} = 0.0087 - 0.0216\alpha_{r,t} + 0.400\alpha_{r,t}^{2} \qquad (1)$$

gives a good approximation of the low Mach number section drag up to angles of attack from $8^{\circ}$ to $10^{\circ}$. At the higher Mach numbers, the angle of attack for drag divergence can generally be easily obtained by calculating the tip angle of attack at the point where the measured-rotor-performance curve initially separates from the low tip Mach number curves. A first estimate of the drag-coefficient rise past drag divergence, based on experience for rotor blades having tip airfoil sections 9 to 15 percent thick, is 0.02 for a Mach number increase of 0.1 past drag divergence.

The section profile-drag coefficients obtained by the aforementioned procedure at the proper Mach number and angle of attack are then inserted into the equations for rotor profile-drag torque, and the rotor profile

torque is then calculated for the various test conditions.  Sufficient
refinement of the synthesized section-profile-drag data is considered to
be obtained when the calculated rotor torque agrees with the measured
data within ±3 percent.


Rotor-Hovering-Performance Analysis

The method used in analyzing the rotor-hovering-performance charac-
teristics is similar to that used in references 2 and 3.  Briefly, this
method shows the onset and rate of growth of the stall and compressibility
drag increases as a function of tip angle of attack and blade mean lift
coefficient.


RESULTS AND DISCUSSION


The synthesized section lift and profile-drag coefficients derived
from the measured rotor performance are presented first, after which the
low tip Mach number maximum lift and high tip Mach number compressibility
effects on the rotor will be discussed and compared with results obtained
with blades having NACA $63_2$-015 and NACA 0015 airfoil sections.

It should be recognized that some of the differences between the
data obtained for blades having different airfoil sections and the dif-
ferences between the synthesized section characteristics obtained from
rotor-blade data and two-dimensional airfoil-section data may be due to
differences in surface condition.  Every effort was made to keep the sur-
faces fair and smooth along the entire blade span and to keep the blade
leading edge (30 percent chord) accurately contoured within (±0.5 percent)
over the outboard half of the rotor-blade radius.


Synthesized Blade-Section Characteristics

Section-lift data.- The synthesized section lift coefficients as a
function of angle of attack and tip Mach number are presented in figure 2.
The curves have been extended beyond the range of the actual test measure-
ments and this area is indicated by the dashed-line curves.  The extensions
are based on probable shapes of the rotor-performance curves past maximum
lift based on previous experience with other rotors.  A comparison of the
synthesized lift coefficients with those obtained from an unpublished two-
dimensional-airfoil investigation made in the Langley low-turbulence pres-
sure tunnel is shown in figure 3.  At a low tip Mach number of 0.3, the
blade-section stall angle obtained from the measured rotor performance
is about $3^\circ$ greater than that shown by the two-dimensional data, and the

blade-section maximum lift coefficient is about 15 percent larger. Similar increments in maximum lift coefficient at low tip Mach numbers have been noted in other tests (refs. 2 and 3). The other principal difference between the two sets of data is a large reduction in lift-curve slope of the synthesized data at a Mach number of 0.8. No explanation for this behavior is as yet available.

Section-profile-drag data.- The synthesized section profile-drag coefficients are shown in figure 4 as a function of Mach number and angle of attack. As with the lift curves, data are presented beyond the actual measurements and this area is indicated by the dashed-line curves. A comparison of the synthesized section profile-drag coefficients with those obtained from the unpublished two-dimensional-airfoil investigation is shown in figure 5. Two principal differences are apparent. The first of these is that at low Mach numbers and high angles of attack (12°) the blade-section data show much lower drag coefficients than the two-dimensional data. This complements the previously discussed lift-coefficient data which indicates that blade-section stall and, thus, the drag rise associated with separated flow would be delayed to an angle of attack about 2° higher than that shown by the two-dimensional data. The other principal difference is the decreased rate of growth of compressibility drag rise at the high Mach numbers compared with that of the two-dimensional-airfoil data. High Mach numbers were obtained only at the tip of the blade, and this decrease in drag coefficient is attributed to the alleviating effects of three-dimensional flow around the blade tip. A similar effect, together with increased values of the drag coefficients below the force break and at low angles of attack (as is also shown in fig. 5), has been pointed out in reference 13 to occur as the aspect ratio of the airfoils tested was reduced from infinity (two-dimensional test) to finite values.

## Rotor Hovering Characteristics

The measured rotor hovering performance over a tip Mach number range from 0.28 to 0.70 is presented in figure 6 as plots of thrust coefficient against torque coefficient. An incompressible rotor-performance curve calculated by using the conventional drag polar (eq. (1)) and by assuming no stall $\left(c_l = a \alpha_{r,t} \text{ and } a = 5.73\right)$ is presented for comparison with the experimental data.

A previous investigation (ref. 14) of a rotor blade having an NACA 0009 airfoil section at the tip indicated a reduction of 5 to 7 percent in rotor maximum thrust at low tip Mach numbers because of wind velocities of 5.2 to 10.4 knots. In order to study this effect on this rotor, data were obtained at wind velocities of 0 and 4.3 to 6.9 knots. The induced torque coefficients have been corrected to the values which would have

been obtained at zero wind velocity by use of the method of reference 15.
The absolute rotor maximum-thrust point was not obtained since the limiting
lag angle of 25° was reached at a collective pitch setting of 18°, and
tests at higher pitch angles were not attempted. As far as the corrected
data go, the effect of wind velocity at tip Mach numbers of 0.28 and 0.32
is a slight increase in rotor profile-drag torque at the highest thrust
coefficients. At higher tip Mach numbers the effects of wind velocity on
profile-drag torque were negligible.

The experimental curve at $M_t = 0.28$ shows good agreement with the
calculated curve up to rotor thrust coefficients of 0.0048 $\left(\overline{c_l} = 0.89\right)$.
The highest blade mean lift coefficient obtained was 1.13. If blade
pitch could have been increased further, a maximum blade mean lift coeffi-
cient about the same (1.15) as that obtained from investigations of rotor
blades having NACA $63_2$-015 (ref. 2) and NACA 0015 (ref. 3) airfoil sec-
tions would be expected.

As the tip Mach number is increased, the same trends that have been
reported in other high tip Mach number investigations are observed, that
is, a progressive reduction in blade mean lift coefficient for drag rise
as tip Mach number is increased. At a tip Mach number of 0.70 the pres-
ent rotor blade has a value of $\overline{c_l}$ of 0.46 for drag divergence
$\left(C_T = 0.0025\right)$ compared with 0.50 for a rotor blade having an NACA
$63_2$-015 airfoil section (ref. 2) and 0.36 for a rotor blade having an
NACA 0015 airfoil section at the tip (ref. 3).

Blade stall patterns near maximum lift.- Blade stall patterns near
maximum lift were obtained by use of a high-speed motion-picture camera
which photographed tufts attached to the blade. The onset and progression
of the separated-flow areas and a calculated spanwise angle-of-attack
distribution for each blade pitch angle are presented in figure 7. The
separated flow has been arbitrarily cut off between the 25- and 30-percent-
radius stations since the camera field of view did not extend further
inboard; however, it is likely that separated flow actually occurred
farther inboard.

Figure 7 shows that separated flow occurs at a calculated section
angle of attack of about 12° inboard and slightly above 13° at the
65-percent-radius station. The high-speed motion pictures indicated
that separated flow initially started over the rearward part of the
airfoil; however, only a slight increase in angle of attack was necessary
to cause separated flow over the entire chord. Also, the separated flow
was intermittent in nature; that is, the flow would separate and reattach
several times per blade revolution.

Rotor-blade efficiency.- The effect of tip Mach number on rotor-
blade efficiency expressed as a figure of merit is shown in figure 8. The
maximum figure of merit at low tip Mach numbers (0.75) agrees with that
obtained with blades having NACA $63_2$-015 and NACA 0015 airfoil sections.
At a tip Mach number of 0.70, the maximum figure of merit of the present
blade dropped to 0.67 as compared with 0.69 for a blade having an NACA
$63_2$-015 airfoil section and with 0.63 for a blade having an NACA 0015 air-
foil section (refs. 2 and 3, respectively).

Effect of tip Mach number on rotor thrust.- Figure 9 shows the varia-
tion of rotor thrust coefficient with blade pitch angle for various tip
Mach numbers. At low tip Mach numbers and at blade pitch settings below
those which produce separated flow, the experimental data agree well with
a calculated curve using a section-lift-curve slope of 5.73. As tip Mach
number is increased, rotor thrust coefficient increases, as would be
expected. A progressive increase in thrust would be expected until lift
divergence occurs. Lift divergence was not obtained, however, with the
present rotor. A previous investigation (ref. 4) of a blade having an
NACA 0012 airfoil at the tip section that was tested to higher tip Mach
numbers indicates that lift divergence occurred between tip Mach numbers
of 0.75 and 0.80.

Rotor-blade pitching moments.- Three different combinations of blade-
tip weight and trailing-edge deflection were tested. Rotor-blade pitching
moments for these three blade configurations are presented in figure 10.
Configuration A (increased tip weight) was used at tip Mach numbers
from 0.28 to 0.52 to reduce the blade lag angle at high pitch settings.
The low tip Mach number curves (0.28 to 0.52) show a stable break (nose
down) as blade mean lift coefficient is increased.

Configurations B and C (normal tip weight; outer 3 feet of blade
trailing edge deflected 0° and 3.5°, respectively) indicate an unstable
(nose up) moment break at tip Mach numbers from 0.62 to 0.70. This
moment break occurs at a slightly lower blade mean lift coefficient than
does drag divergence. Data presented in reference 4 on pitching moments
of blades having an NACA 0012 airfoil section at the tip indicated a
similar moment trend, but the moment break was delayed to blade mean lift
coefficients past drag divergence. At higher tip Mach numbers (0.74
to 0.83), reference 4 shows little change in pitching moment as a function
of blade mean lift coefficient. Evidently, for this airfoil at tip Mach
numbers and blade mean lift coefficients near drag divergence, a small
forward shift of center of pressure occurs. At Mach numbers beyond drag
divergence, the center of pressure appears to shift rearward again.

Rotor Profile-Drag Torque

The principal effect of stall and compressibility has been shown (refs. 2, 3, and 14) to be a rapid increase in rotor profile-drag torque. Figure 11 presents the rate of growth of rotor profile-drag torque coefficients as a function of calculated tip angle of attack for various tip Mach numbers. The results show the same general trend of progressive reduction in tip angle of attack for drag divergence as has been shown in previous investigations. It should be noted that, at low tip Mach numbers, the drag rise should be associated with the angles of attack for separated flow (fig. 7) rather than with the tip angle of attack.

Another method of showing the drag rise and one that offers a better comparison of overall rotor performance is afforded by plotting the ratio of profile-drag torque coefficients as a function of blade mean lift coefficient at various tip Mach numbers as in figure 12. At low tip Mach numbers the blade mean lift coefficient of the present rotor blade at drag rise was about the same as that obtained in tests of a blade having an NACA $63_2$-015 airfoil section and was about 10 percent lower than that obtained with a blade having an NACA 0015 airfoil section. At the high tip Mach numbers (0.70), the NACA 0012 and NACA $63_2$-015 airfoil sections have blade mean lift coefficients of 0.46 and 0.50, respectively, at drag divergence. The blade mean lift coefficient for drag divergence obtained for a blade having an NACA 0015 airfoil section is about 25 percent less (ref. 3).

Comparison of Rotor Drag-Divergence Data

With Two-Dimensional-Airfoil Data

The variation of the measured rotor-blade-tip drag-divergence Mach numbers with the angles of attack calculated for the blade-tip station is shown in figure 13. The present data curve is compared with two curves based on two-dimensional-airfoil data. For one curve, the drag-divergence Mach number is defined as the point at which the variation of $c_{d,o}$ with M at a given angle of attack reaches a slope $\frac{\Delta c_{d,o}}{\Delta M}$ of 0.1. For the other curve, the drag-divergence Mach number of the airfoil section is taken as the point at which the drag coefficient first shows an increase over its incompressible value. The latter method is similar to the method in which the experimental rotor drag-rise points were obtained.

The rotor experimental results show the same trends as those obtained from an investigation of a blade with an NACA 0012 airfoil section at the tip (ref. 4). At high tip Mach numbers, the drag rise is delayed to a tip angle of attack about $2^\circ$ higher than that indicated by two-dimensional-airfoil data. At low tip Mach numbers the drag rise occurs at lower tip

angles of attack than those shown by the two-dimensional results. As previously explained, this drag rise should be associated with the angle of attack for separated flow occurring over the inboard regions of the blade (12° to 13°) rather than with the tip angle of attack of 9°.

CONCLUDING REMARKS

Rotor-blade section lift and profile-drag characteristics for an NACA 0012 airfoil have been synthesized for use in calculations of helicopter-rotor hovering performance. Rotor hovering performance from which the major portion of the synthesized data was derived is presented for tip Mach numbers from 0.28 to 0.70. The synthesized data presented for Mach numbers from 0.70 to 0.88 were derived from a previous investigation of another blade having an NACA 0012 airfoil section at the tip.

At low tip Mach numbers, the synthesized data show higher maximum lift coefficients and lower profile-drag coefficients at maximum lift coefficient than do the two-dimensional-airfoil data. At high tip Mach numbers, the rate of increase in drag coefficient past drag divergence is less than that shown by two-dimensional-airfoil data.

The rotor hovering performance as a function of tip Mach number follows the same general pattern as that established by previous investigations of high tip Mach numbers; that is, a large increase occurs in profile-drag torque once the critical combination of tip angle of attack and tip Mach number for drag divergence is exceeded.

Langley Aeronautical Laboratory,
        National Advisory Committee for Aeronautics,
                Langley Field, Va., July 1, 1958.

REFERENCES

1. Gessow, Alfred:  Equations and Procedures for Numerically Calculating
   the Aerodynamic Characteristics of Lifting Rotors.  NACA TN 3747,
   1956.

2. Shivers, James P., and Carpenter, Paul J.:  Experimental Investigation
   on the Langley Helicopter Test Tower of Compressibility Effects on
   a Rotor Having NACA $63_2$-015 Airfoil Sections.  NACA TN 3850, 1956.

3. Shivers, James P., and Carpenter, Paul J.:  Effects of Compressibility
   on Rotor Hovering Performance and Synthesized Blade-Section Charac-
   teristics Derived From Measured Rotor Performance of Blades Having
   NACA 0015 Airfoil Tip Sections.  NACA TN 4356, 1958.

4. Powell, Robert D., Jr.:  Compressibility Effects on a Hovering Heli-
   copter Rotor Having an NACA 0018 Root Airfoil Tapering to an NACA
   0012 Tip Airfoil.  NACA RM L57F26, 1957.

5. Loftin, Laurence K., Jr., and Smith, Hamilton A.:  Aerodynamic Charac-
   teristics of 15 NACA Airfoil Sections at Seven Reynolds Numbers
   From $0.7 \times 10^6$ to $9.0 \times 10^6$.  NACA TN 1945, 1949.

6. Critzos, Chris C., Heyson, Harry H., and Boswinkle, Robert W., Jr.:
   Aerodynamic Characteristics of NACA 0012 Airfoil Section at Angles
   of Attack From $0^\circ$ to $180^\circ$.  NACA TN 3361, 1955.

7. Abbott, Ira H., Von Doenhoff, Albert E., and Stivers, Louis S., Jr.:
   Summary of Airfoil Data.  NACA Rep. 824, 1945.  (Supersedes NACA
   WR L-560.)

8. Wilson, Homer B., Jr., and Horton, Elmer A.:  Aerodynamic Character-
   istics at High and Low Subsonic Mach Numbers of Four NACA 6-Series
   Airfoil Sections at Angles of Attack From $-2^\circ$ to $31^\circ$.  NACA
   RM L53C20, 1953.

9. Graham, Donald J., Nitzberg, Gerald E., and Olson, Robert N.:  A
   Systematic Investigation of Pressure Distributions at High Speeds
   Over Five Representative NACA Low-Drag and Conventional Airfoil
   Sections.  NACA Rep. 832, 1945.

10. Racisz, Stanley F.:  Effects of Independent Variations of Mach Number
    and Reynolds Number on the Maximum Lift Coefficients of Four NACA
    6-Series Airfoil Sections.  NACA TN 2824, 1952.

11. Gessow, Alfred:  Effect of Rotor-Blade Twist and Plan-Form Taper on
    Helicopter Hovering Performance.  NACA TN 1542, 1948.

12. Bailey, F. J., Jr.: A Simplified Theoretical Method of Determining the Characteristics of a Lifting Rotor in Forward Flight. NACA Rep. 716, 1941.

13. Stack, John, and Lindsey, W F.: Characteristics of Low-Aspect-Ratio Wings at Supercritical Mach Numbers. NACA Rep. 922, 1949. (Supersedes NACA TN 1665.)

14. Powell, Robert D., Jr., and Carpenter, Paul J.: Low Tip Mach Number Stall Characteristics and High Tip Mach Number Compressibility Effects on a Helicopter Rotor Having an NACA 0009 Tip Airfoil Section. NACA TN 4355, 1958.

15. Carpenter, Paul J.: Effect of Wind Velocity on Performance of Helicopter Rotors As Investigated With the Langley Helicopter Apparatus. NACA TN 1698, 1948.
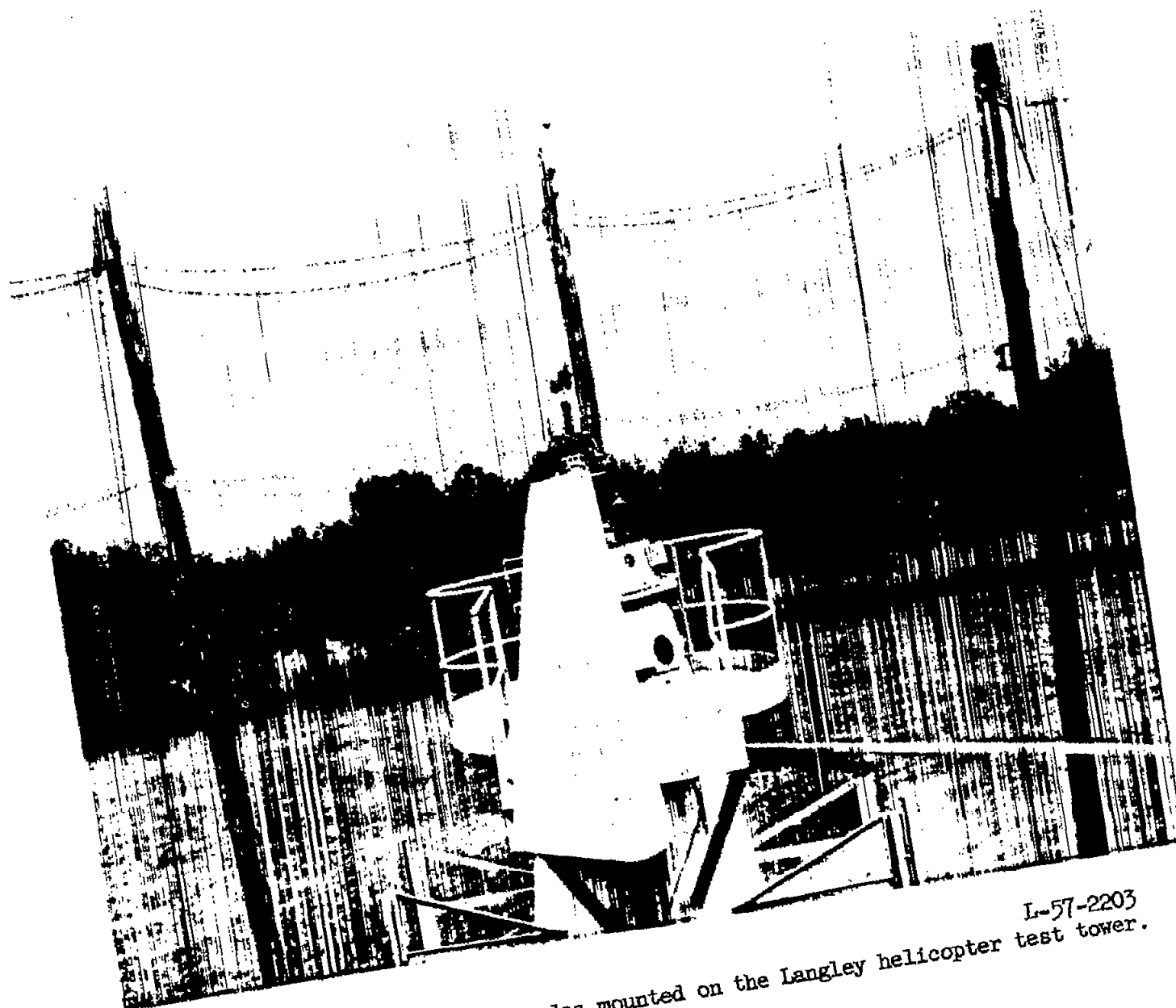
Figure 1.-- View of rotor blades mounted on the Langley helicopter test tower.

L-57-2203
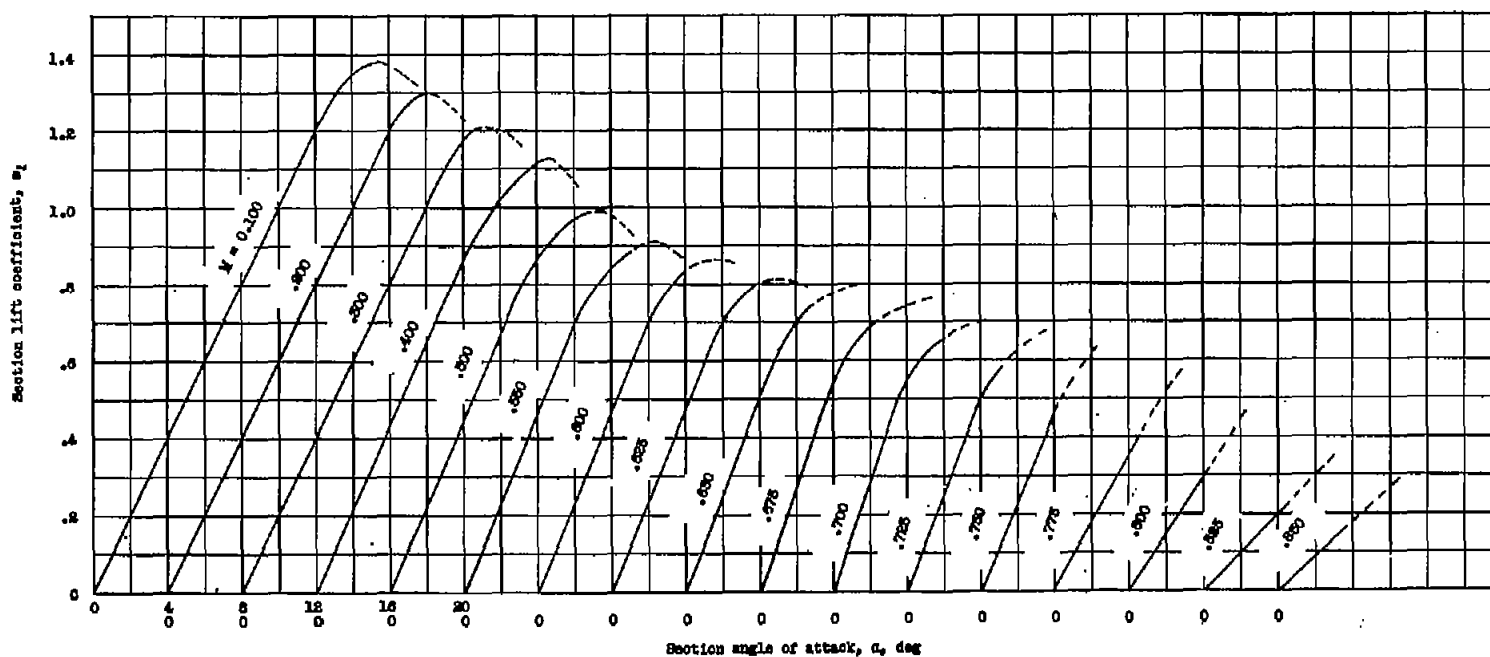
Figure 2.- Variation of synthesized section lift coefficient with angle of attack at various Mach numbers for an NACA 0012 airfoil section.
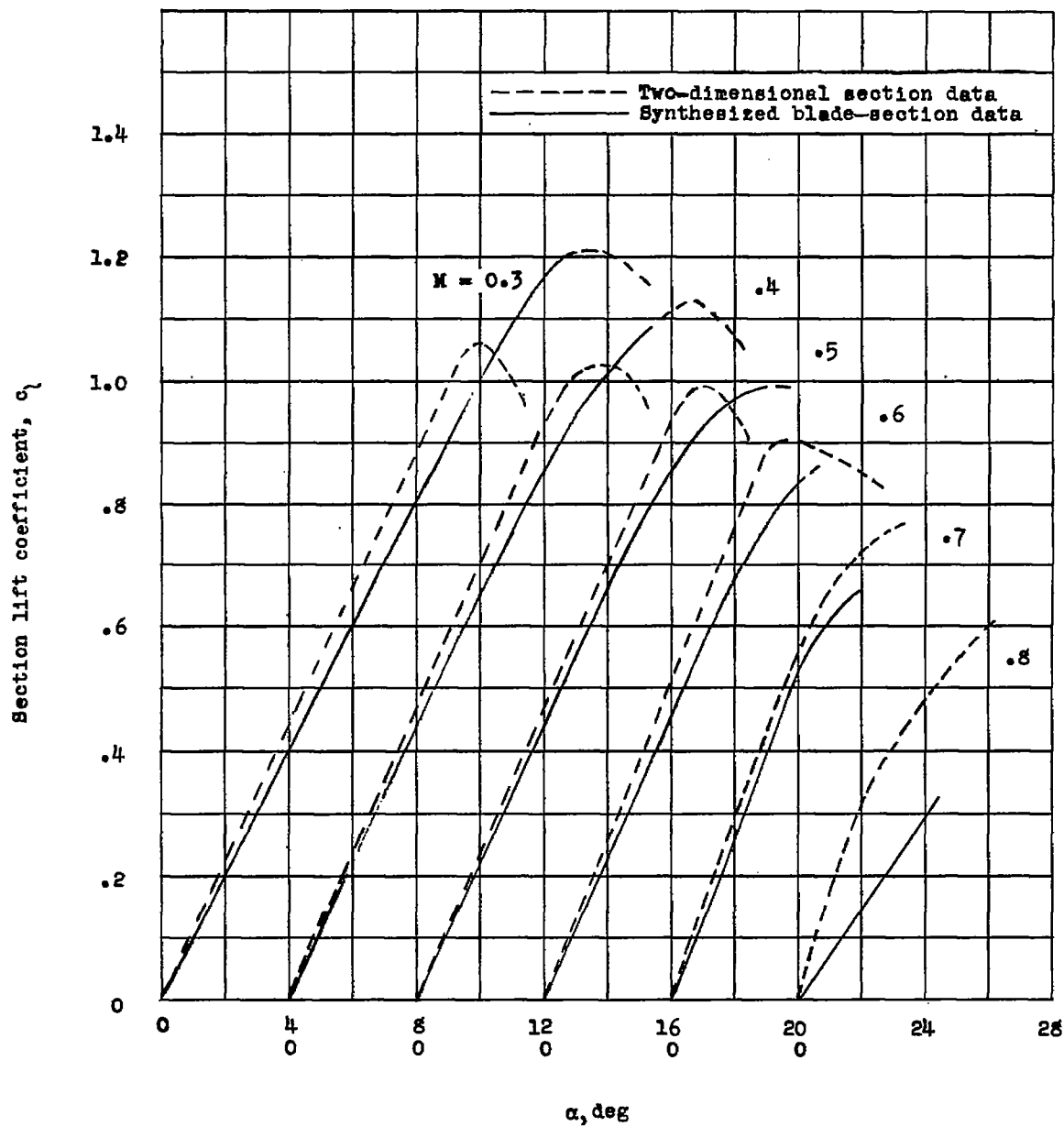
Figure 3.- Comparison of two-dimensional and synthesized blade-section
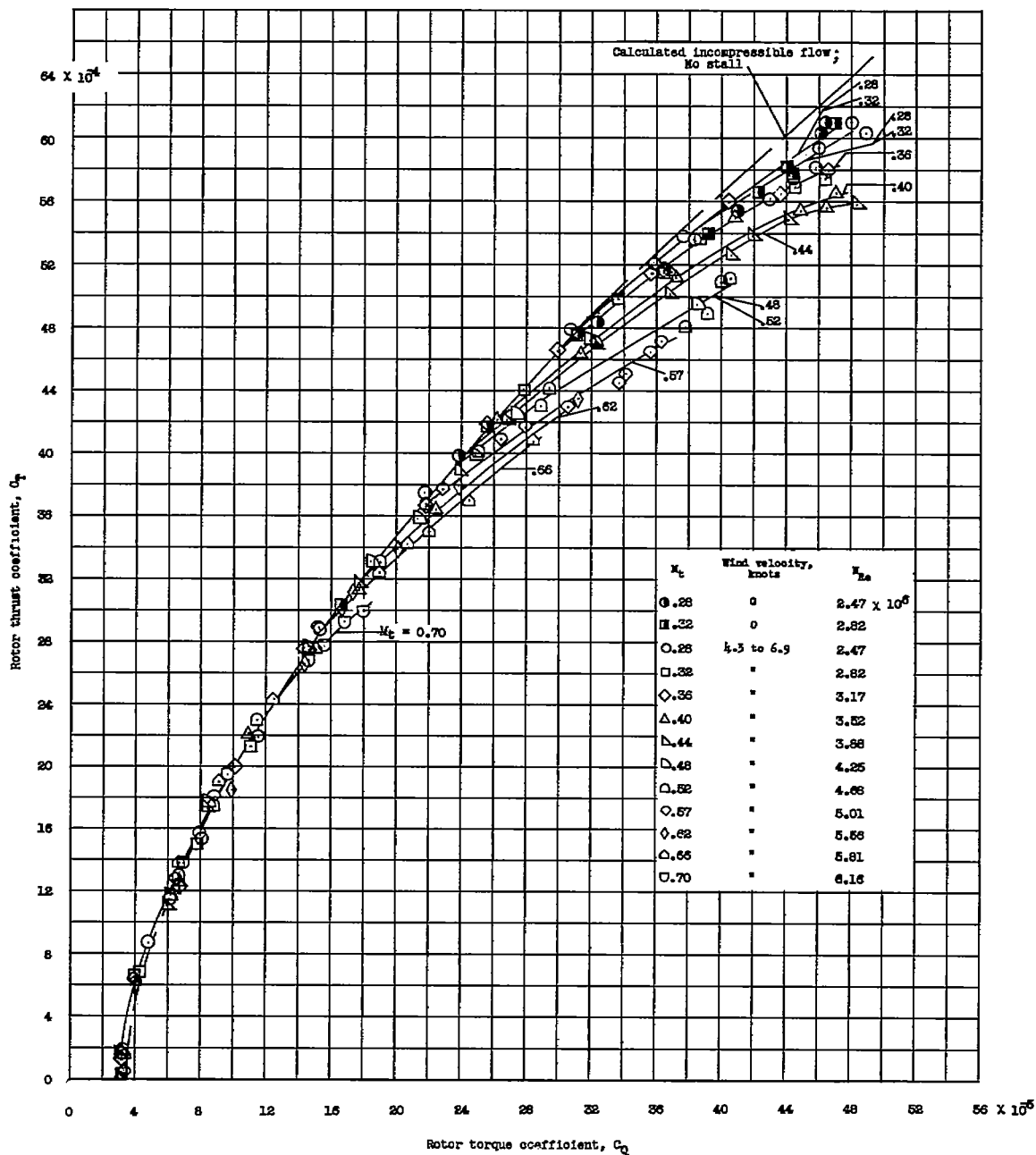lift characteristics for NACA 0012 airfoil section.
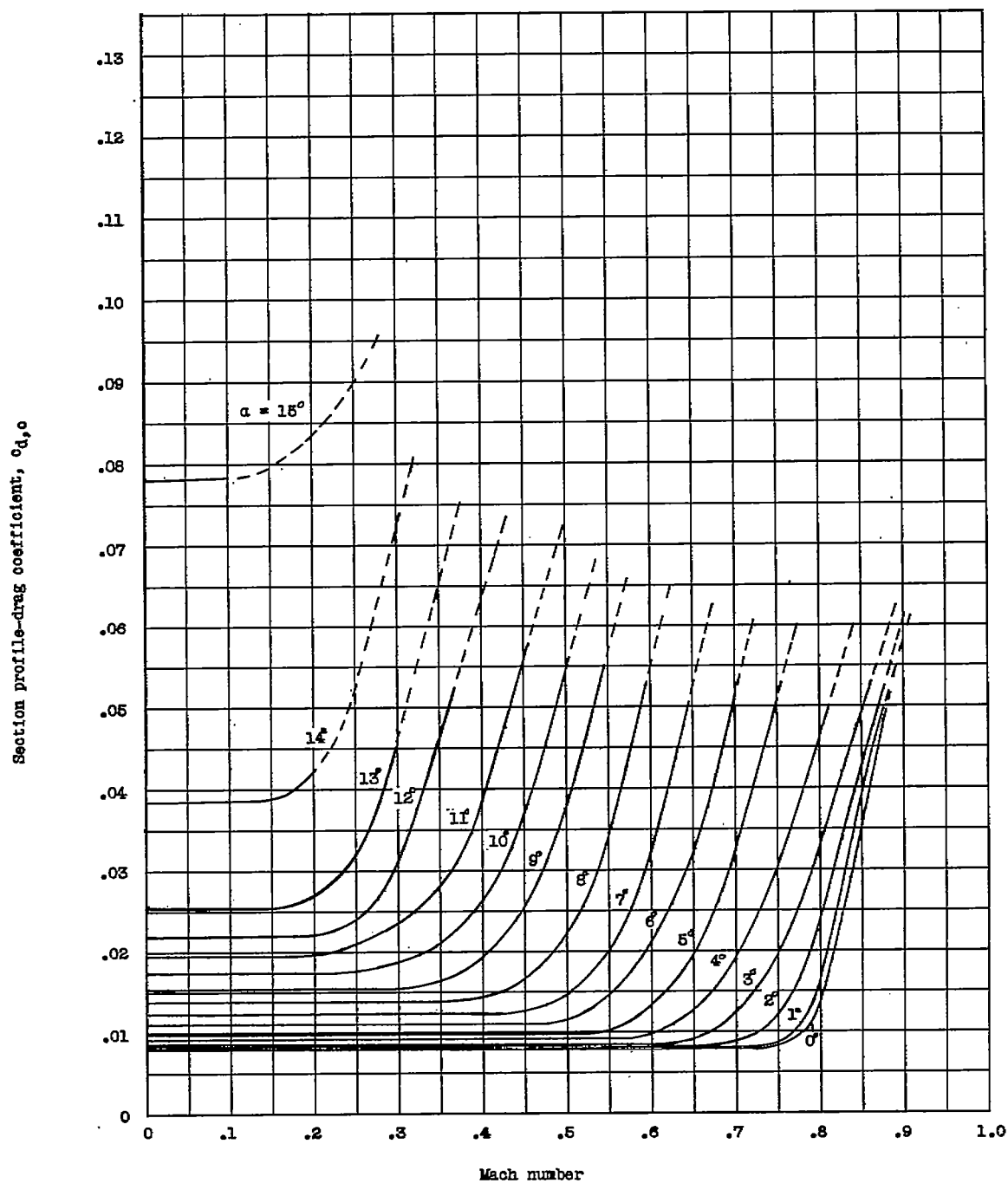
Figure 4.- Variation of synthesized section profile-drag coefficient with
Mach number at various angles of attack for an NACA 0012 airfoil
section.
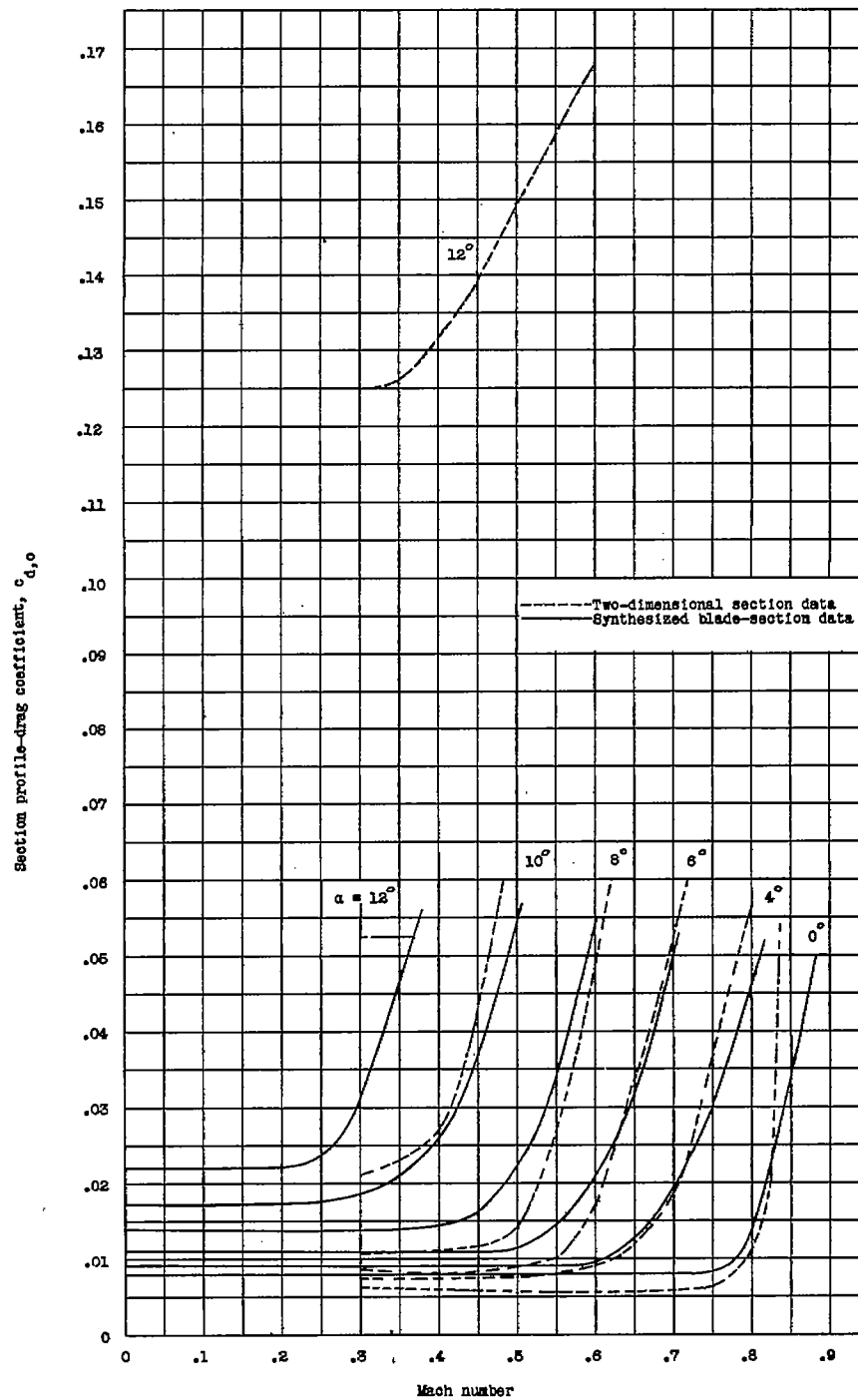
Figure 5.- Comparison of two-dimensional and synthesized blade-section
      profile-drag characteristics for NACA 0012 airfoil section.

Figure 6.- Hovering performance of rotor blades having an NACA 0012 air-
foil section throughout blade span. Calculated curve based on equa-
tion (1) and no stall $\left(c_l = a\alpha_{r,t}\right)$; σ = 0.0325; induced torque
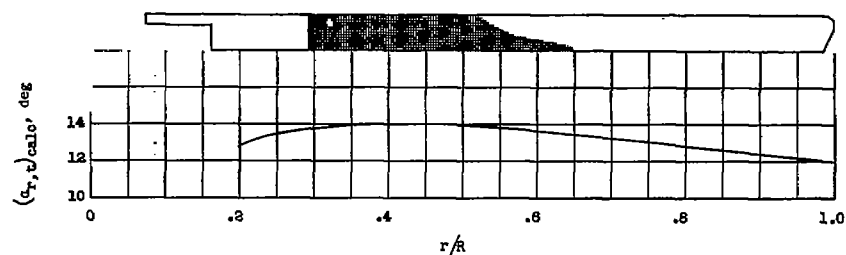coefficients have been corrected to zero-wind condition.
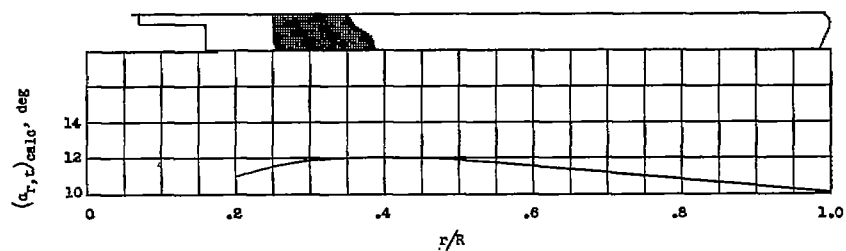
(a)   $\theta_{0.75R} = 15.3^{\circ}$;  $\overline{c_l} = 0.99$.
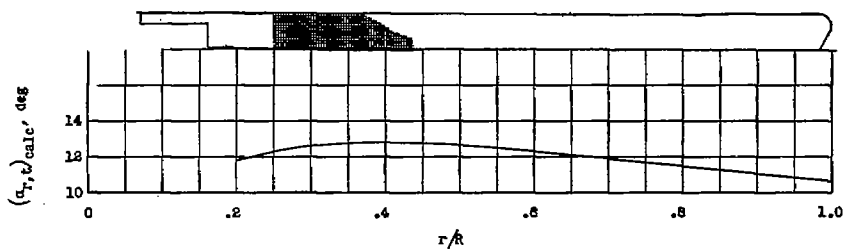


(b)   $\theta_{0.75R} = 16.2^{\circ}$;  $\overline{c_l} = 1.04$.
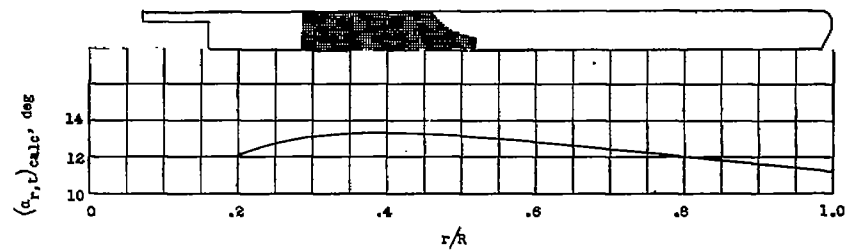


(c)   $\theta_{0.75R} = 16.7^{\circ}$;  $\overline{c_l} = 1.06$.



(d)   $\theta_{0.75R} = 17.9^{\circ}$;  $\overline{c_l} = 1.12$.

Figure 7.- Progression of intermittent flow separation on rotor blade as pitch is increased (as indicated by tuft patterns).  $M_t = 0.28$; $N_{Re} = 2.5 \times 10^6$.
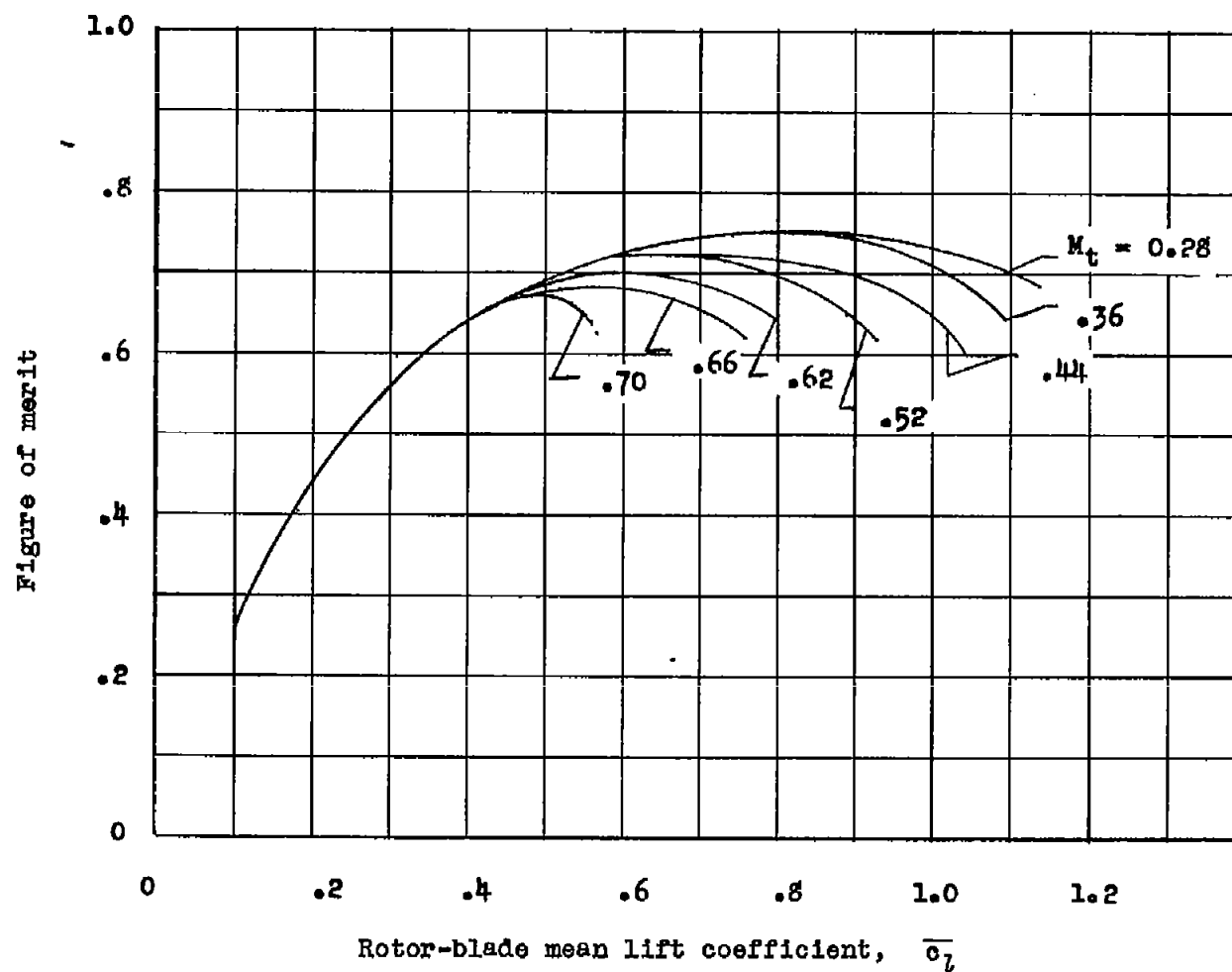
Figure 8.- Effect of tip Mach number on rotor-blade figure of merit $\left(0.707 \dfrac{C_T^{3/2}}{C_Q}\right)$.
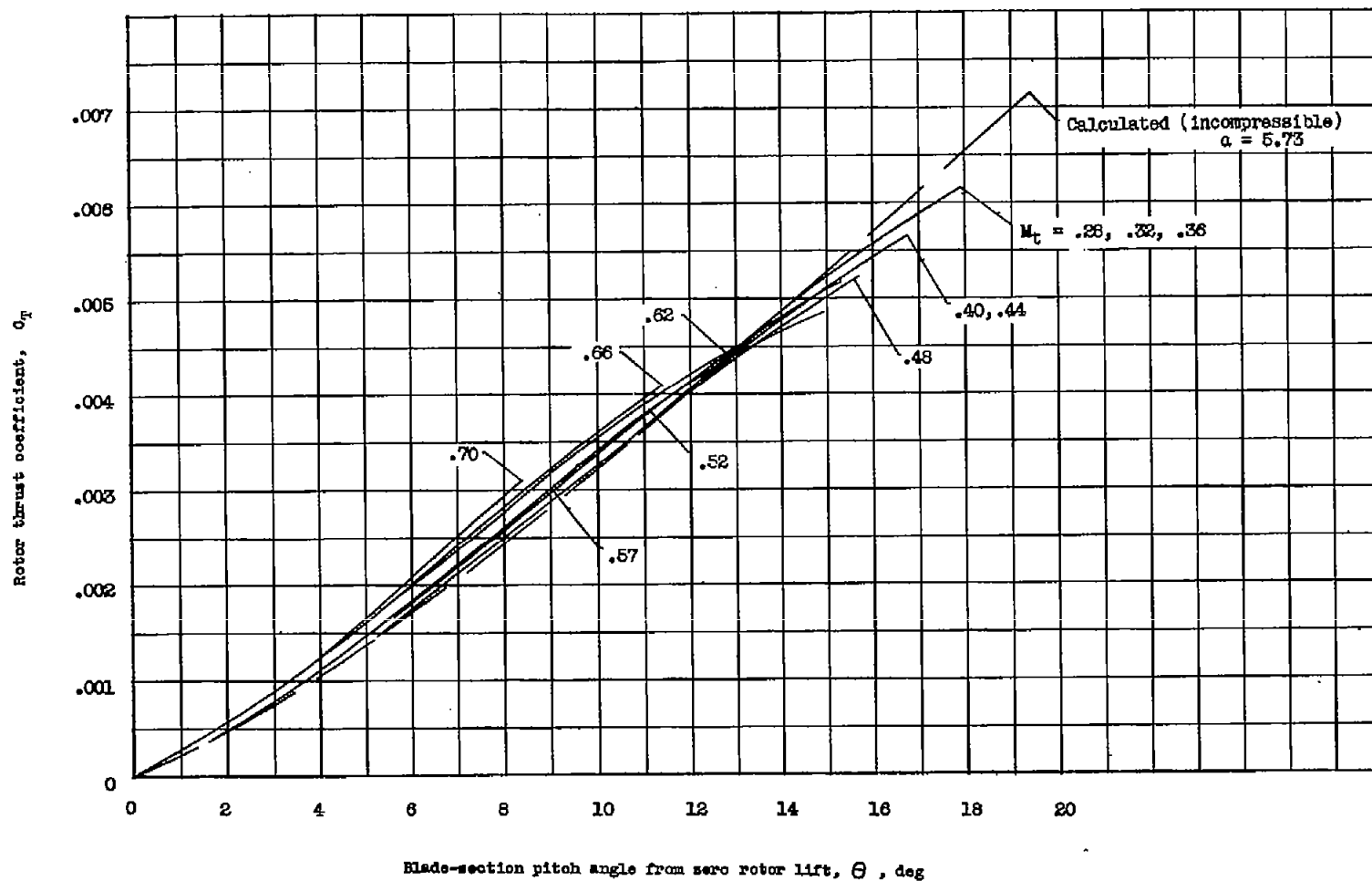
Figure 9.- Variation of rotor thrust coefficient with blade-section
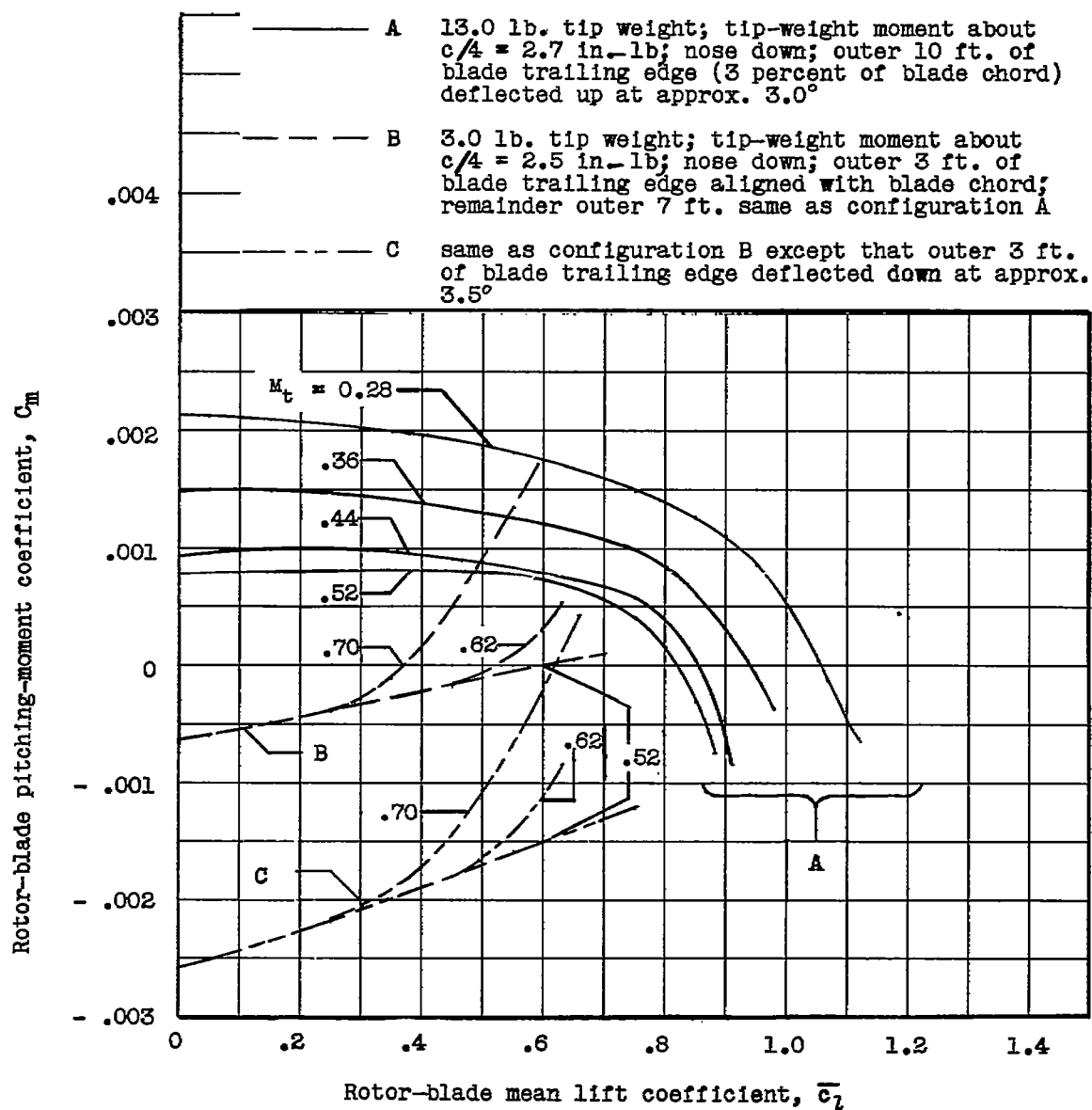pitch angle for various tip Mach numbers.

A    13.0 lb. tip weight; tip-weight moment about
     c/4 = 2.7 in.-lb; nose down; outer 10 ft. of
     blade trailing edge (3 percent of blade chord)
     deflected up at approx. 3.0°

B    3.0 lb. tip weight; tip-weight moment about
     c/4 = 2.5 in.-lb; nose down; outer 3 ft. of
     blade trailing edge aligned with blade chord;
     remainder outer 7 ft. same as configuration A

C    same as configuration B except that outer 3 ft.
     of blade trailing edge deflected down at approx.
     3.5°



Figure 10.- Effect of tip Mach number, tip weight, and blade trailing-
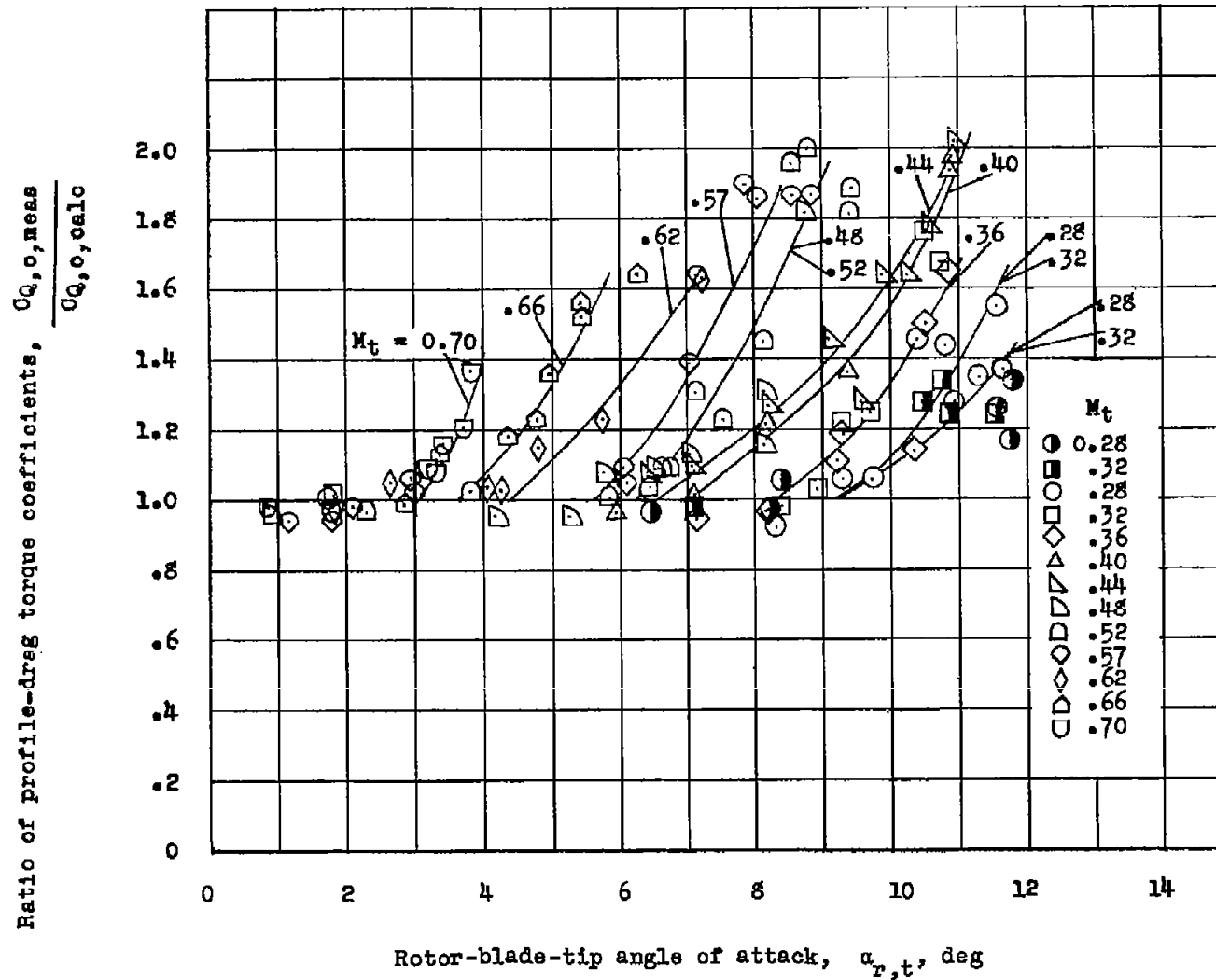edge deflection on rotor-blade pitching moments.

Figure 11.- Effect of tip Mach number and tip angle of attack on profile-drag torque ratio. Half-darkened symbols indicate data obtained at zero-wind velocity.
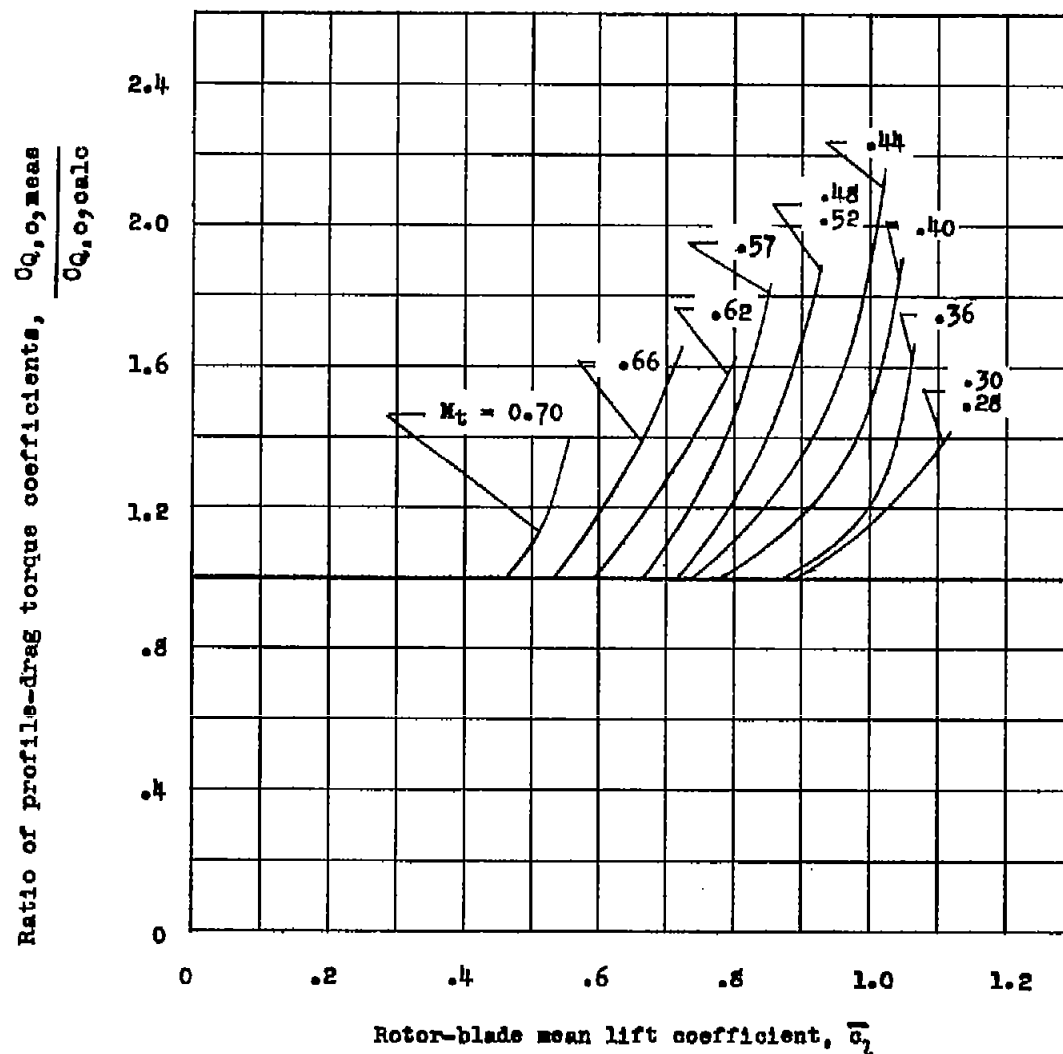
Figure 12.- Effect of tip Mach number and blade mean lift coefficient on profile-drag torque ratio of rotor blade.
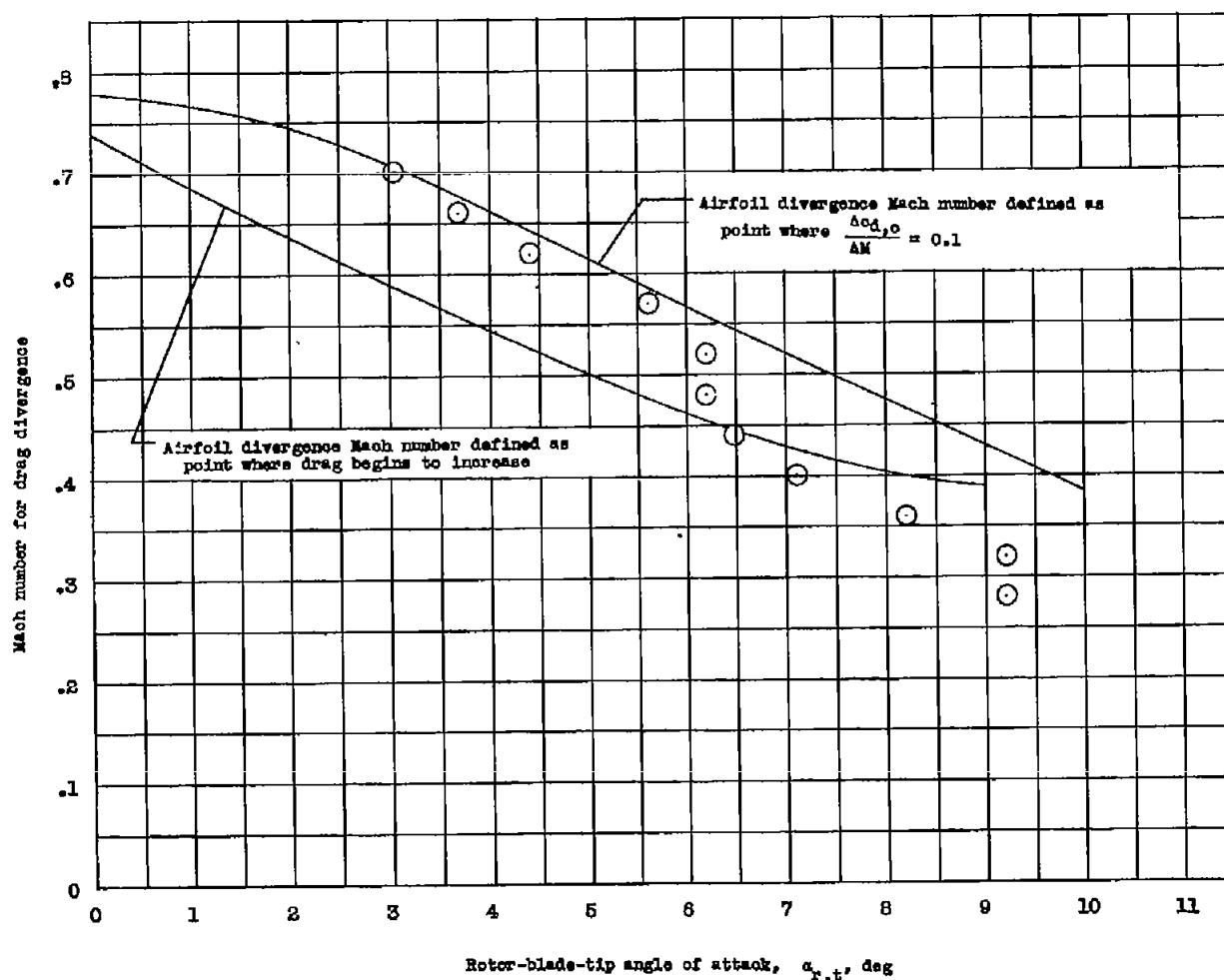
Figure 13.- Comparison of two-dimensional-airfoil drag-divergence data
with rotor experimental data. Curves are from unpublished two-
dimensional-airfoil data for NACA 0012 airfoil section; symbols
represent $M$ and $\alpha_{r,t}$ at which experimental data from the rotor
blade separate from the curve calculated by using the airfoil drag
polar given in equation (1).